

MILLING-INDUCED AMORPHIZATION IN A CHALCOGENIDE COMPOUND

A. QIAO^a, H. YANG^a, H. Y. XIAO^a, J. XIAO^{a*}, X. P. LIU^b, Z. R. GE^b,
R. H. CHEN^b

^aState Key Laboratory of Silicate Materials for Architectures, Wuhan University of Technology, Wuhan 430070, China.

^bJiangsu Ruihe Abrasives co., Ltd., Yancheng 224051, Jiangsu, China

The mechanism of milling-induced amorphization was studied by investigating the structural evolution during amorphization via high-energy ball milling of a chalcogenide compound, i.e. Ag₃PS₄ crystal. The gradual decrease in intensity of the XRD diffraction peaks of Ag₃PS₄ milled for different durations indicates that the degree of amorphization was enhanced by the mechanical milling. The forward shift and evolution of the bimodal crystallization peak investigated by differential scanning calorimetry (DSC) imply that amorphization occurs from the surface state and extends to the bulk state until complete amorphization of the entire material. Furthermore, the Ag K-edge extended X-ray absorption fine structure (EXAFS) spectra manifest that during the milling, the Ag-S bonds in the Ag₃PS₄ crystal were broken firstly. Then, the distribution of Ag-S bond angles became wider and the coordination structure became more disordered with longer durations of mechanical milling.

(Received March 29, 2017; Accepted May 23, 2017)

Keywords: High energy ball-milling, Amorphization, Amorphous Ag₃PS₄

1. Introduction

Solid ionic electrolytes (SIEs) have attracted much attention due to their high ion conductivities and non-flammability.^{1,2} SIEs can be used in safe, all-solid state batteries, which are promising candidates for future applications by replacing present commercial batteries which use organic or liquid electrolytes.³ The amorphous or glass-ceramic ionic conductors are among the most promising electrolytes, because they possess equivalent or higher ionic conductivity compared to their crystalline analogs.⁴⁻⁷ The amorphous ionic conductors can be prepared via many routes, such as melt-quenching, vapor deposition, sputtering, high energy ball-milling and so on.⁸ Among these techniques, the high energy ball-milling or mechanical milling is a new and effective preparation procedure for inorganic amorphous conductors with high ionic conductivity.^{9,10} The glassy powders can be obtained via a relatively simple high energy ball milling process at ambient temperature and the milled powders can be directly used as solid electrolytes. Most important of all, this technique can be utilized to synthesize some novel and highly active amorphous materials which cannot be obtained by conventional methods, such as the melt quenching method.^{11,12}

While there has been considerable progress in studying the milling process of crystalline materials,¹³⁻¹⁵ the mechanism of the milling-induced amorphization is not yet well understood, due to the complex milling process and its mechanical effects involved in impact, friction, shear, etc. as well as the thermal effect, i.e. rise in local temperature. It has been generally accepted that numerous structural defects are created and strain is introduced into the lattice during mechanical milling of the crystal.¹⁶ As a result, crystals fracture into smaller and smaller pieces. Furthermore, the lattice structure is disordered due to the accumulation of defects and strain, thus the amorphous structure is formed. However, how does amorphization occur in the particles during milling and how does the microstructure evolve during the crystalline-to-amorphous transformation? In this

work, we attempted to answer these two questions insight from the milling-induced process of a chalcogenide compound, i.e. Ag_3PS_4 .

First, we prepared Ag_3PS_4 crystals according to the previously reported procedures,¹⁷ whose amorphous version has not yet been obtained to the best of our knowledge. Then, the amorphous Ag_3PS_4 was prepared from the Ag_3PS_4 crystal via high energy ball-milling technique. Second, the phase structure and calorimetric behavior of the samples milled for different durations were investigated by X-ray diffraction (XRD) and differential scanning calorimetry (DSC) methods. Finally, the evolution of coordination structure was monitored by the Ag K-edge extended X-ray absorption fine structure (EXAFS) spectra. Exploring the formation process and the structural evolution of amorphous Ag_3PS_4 by milling Ag_3PS_4 glasses is of great importance for understanding the nature of the mechanical milling-derived amorphization, as well as of great practical interest for improving the properties of ionic conductors synthesized by milling.

2. Experimental procedure

The Ag_3PS_4 crystal was prepared by a melt-cooling method. The mixture of reagent-grade Ag_2S and P_2S_5 (all from Aladdin) with a molar ratio 3:1 was put into a 10mm inner diameter silica tube, sealed under a vacuum of 10^{-2} Pa, melted at 1173 K in a rocking furnace, reduced to 873 K and kept at this temperature for 20h, then naturally cooled down to room temperature. Through this procedure, high pure Ag_3PS_4 crystal phase was obtained as confirmed by room-temperature powder X-ray diffraction (PXRD) data in Fig.1 (curve A). Subsequently, using a high-energy ball mill (Fritsch, Pulverisette-7 premium line), the as-prepared Ag_3PS_4 crystals were milled at 600 rpm for different duration (2~20h). More details about the sample preparation can be found in our previous work.

Using Cu K_α ($\lambda=1.540598$ Å) radiation, PXRD data were collected with a Rigaku-RU 200B diffractometer. The calorimetric measurements were carried out using a Netzsch STA 449 F1 instrument in an argon atmosphere. The samples were placed in a platinum crucible situated on a sample holder of the differential scanning calorimeter (DSC) at room temperature and subjected to up-scans at 10 K/min to 623 K. The Ag K-edge EXAFS spectra were collected in transmission mode at the beam lines BL14W1 (Shanghai Synchrotron Radiation Facility of China). A Si(311) double crystal monochromator was used to obtain a monochromatic X-ray beam from the 3.5 GeV electron storage ring with a current between 150–210 mA. EXAFS data were processed by a software package IFEFFIT.¹⁸

3. Results

As seen from curve A in Fig. 1, only the characteristic peaks ascribed to Ag_3PS_4 crystalline phase (JCPDS 47-1173) can be detected for the melt-cooled sample, indicating that very pure crystalline Ag_3PS_4 can be obtained by the melt-cooling method. On the other hand, for the milled Ag_3PS_4 samples, the sharp X-ray diffraction peak disappeared and a broad diffraction peak appeared, indicating the presence of the amorphous phase. Although the main phase is amorphous for the samples milled for 2-6 h, some small diffraction peaks can be seen, indicating that some crystalline domains still existed. After 10 h of milling, the crystalline Ag_3PS_4 was amorphized completely. Therefore, the amorphization or the disordering of Ag_3PS_4 crystal occurred gradually with increasing duration of mechanical milling, and the amorphous Ag_3PS_4 can be achieved by mechanical milling for 10 h.

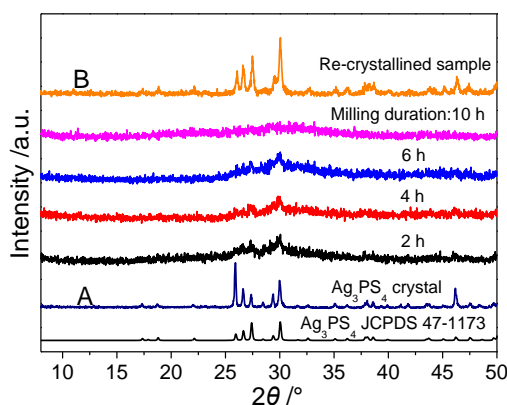


Fig.1 XRD patterns of the Ag_3PS_4 crystal, the Ag_3PS_4 powder as-milled for different durations, together with the re-crystallized sample, i.e. the Ag_3PS_4 powder as-milled for 10h previously, which was further subjected to a heat-treatment at 530K for 10 min.

An obvious crystallization peak was observed in the DSC curves (Fig. 2) for each of the milled samples, in contrast to the flat DSC curve for the Ag_3PS_4 crystal. When the sample milled for 10 h was annealed at 530 K for 10 min, the crystalline Ag_3PS_4 was obtained again (see curve B, Fig. 1). With the extension of milling duration, the onset of crystallization peak (T_{onset}) shifted towards higher temperature and the crystallization enthalpy (ΔH) increased, as shown in the inset of Fig. 2. The detailed changes in temperature and energy release during the milling process are shown in Table 1. All these data indicate that the degree of amorphization was enhanced by longer period of mechanical milling. Although the as-milled Ag_3PS_4 sample is glassy, its DSC up-scan curve does not exhibit a glass transition peak prior to the sharp exothermic crystallization (Fig. 2). This is likely because the glass transition peak is masked by the crystallization peak.

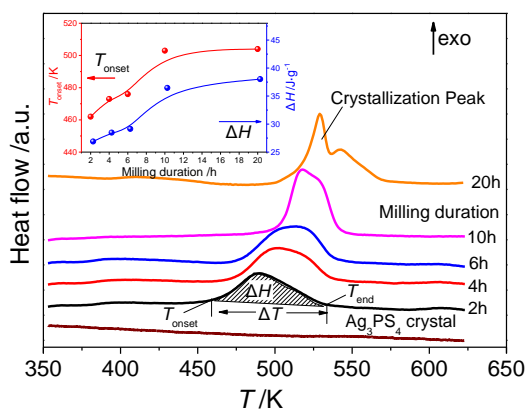


Fig.2 DSC up scans of the Ag_3PS_4 crystal and the Ag_3PS_4 powder as-milled for different durations.

Table 1. Characteristic temperatures, total enthalpy release (ΔH) during the crystallization for the Ag_3PS_4 powder as-milled for different durations.

Milling time t/h	$T_{\text{onset}}/\text{K}$	T_{end}/K	$\Delta T/\text{K}$	$\Delta H/\text{J}\cdot\text{g}^{-1}$
2	462	540	78	26.89
4	473	549	76	28.48
6	476	550	74	29.14
10	503	558	55	36.46
20	504	575	71	32.56

T_{onset} , the onset temperature of crystallization peak; T_{end} , the end temperature of crystallization peak;

$$\Delta T = T_{\text{end}} - T_{\text{onset}}$$

Furthermore, the local coordination structures for the crystalline and milled Ag_3PS_4 samples were investigated by EXAFS with Ag K-edge. Fig. 3 depicts the k^2 -weighted EXAFS function, $k^2\chi$, where k and χ are the wavenumber and normalized EXAFS signal, respectively. $k^2\chi$ was obtained with good resolution up to k of 12 \AA^{-1} for crystalline Ag_3PS_4 and the Ag_3PS_4 samples milled for different durations. Fourier transforms of the $k^2\chi$ functions were calculated for the k -range from 2.0 to 12.0 \AA^{-1} with a Hanning-type window function.

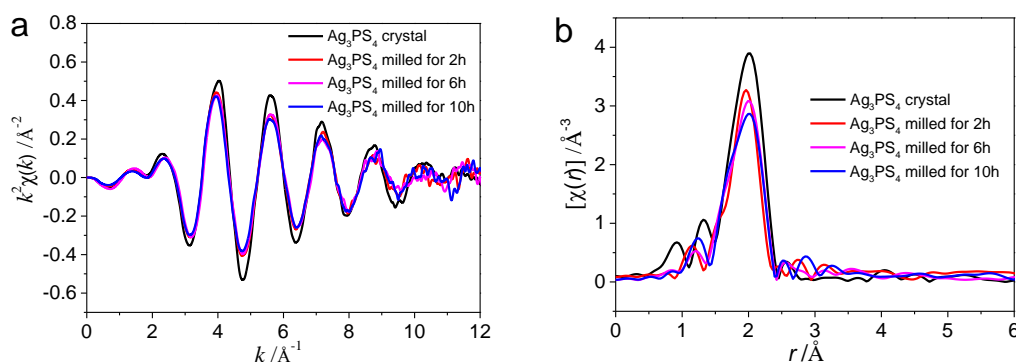


Fig.3 Ag K-edge EXAFS spectra of the Ag_3PS_4 crystal and the Ag_3PS_4 powder as-milled for different durations. (a) EXAFS signal in $k^2\chi(k)$ form. (b) Fourier transform

4. Discussion

After only 2 h of milling, a majority of the ordered structure of the crystalline Ag_3PS_4 is broken by the mechanical milling process, though some crystalline parts can still be detected (Fig. 1). When subjected to 10 h of milling, all the crystalline powder was amorphized. However, there was no obvious damping in the intensity of diffraction peaks of the milled samples having some remaining crystalline regions, which could be due to the sensitivity limitation of XRD measurement. The detailed process of amorphization along with the increase in milling duration can be inferred from the crystallization behavior. It can be seen from Table 1 and the inset of Fig. 2 that increasing the milling time (t) leads to an increase in the crystallization enthalpy (ΔH). When milling is continued for more than 10 h, the ΔH further increases and then almost remains constant. The ΔH , the total energy release during crystallization, is directly related to the proportion of amorphous parts of the sample.¹⁹ So the increase in ΔH value indicates that the crystalline parts decrease as the milling time increases until they completely vanish. When the t is up to 10 h, the amorphization of the entire material is completed. Therefore, the mechanical milling is a gradual process to amorphize the crystalline Ag_3PS_4 . The shifting forward of T_{onset} indicates that the degree of amorphization was enhanced by the mechanical milling.²⁰

We then analyzed how this gradual amorphization proceeds. Herein, we propose that the surface is firstly amorphized followed by the bulk part. This hypothesis can be explained by the following analysis. The mechanical milling is typically an “up to down” process,²¹ i.e., it decreases the particle size and increases the grain boundary area. Thus, the proportion of surface state is dramatically increased, and extra free energy and defects are induced on the surface. So the active and defective surface is likely to be amorphized first, followed by the bulk as the milling time increases, which could be confirmed by the crystallization behavior of the sample milled for different durations (Fig. 2). The asymmetrical crystallization peaks in the DSC curves provide evidence for the non-isothermal crystallization pattern, indicating the highly heterogeneous structure of the milled Ag_3PS_4 .²² The presence of the bimodal peak could be explained by the defect-induced surface crystallization followed by nuclei-induced bulk crystallization. The extent of the latter part of bimodal peak appears to be enhanced by raising t from 2 h to 6 h. It could be because the milling induces more and more bulk crystalline parts to become amorphous, resulting in a larger region of amorphous bulk. When the duration of the milling is sufficiently long (10 h and 20 h), the former part of the bimodal peak becomes more dominant, because in absolutely amorphous state, the milling will cause the surface state to be more active and defective. Furthermore, when milling for 10 h, the ΔT , which corresponds to crystal growth originating dominantly from the glass with heterogeneities,²³ reaches a minimum (Table 1), indicating that is less heterogeneity in the amorphous Ag_3PS_4 . So upon insufficient milling, the structural heterogeneity, i.e. mixture of surface amorphous state with bulk crystalline state, is dominant. On the other hand, when there is sufficient milling, the energetic heterogeneity, i.e. the highly excited surface and less excited bulk, is pronounced. Moreover, the structural heterogeneity in the 2 h to 10 h milled samples leads to heterogeneous nucleation, i.e. the amorphous surface is crystallized induced by the bulk crystallinity. With the increase in milling time, the proportion of the bulk crystal decreases rapidly, lowering the effect of heterogeneous nucleation. Thus, the T_{onset} shifts forward with the increase in milling time.

Further information on the coordinating species was obtained by EXAFS. As shown in Fig. 3, a peak at the same position around 2.5 Å was observed, which is attributed to the Ag-S bond. With the increase in milling time, the intensity of the peak at 2.5 Å decreases. The peak intensity is affected by coordination number and distribution of coordination distance.²⁴ In crystalline materials, the intensity decrease is primarily derived from the decrease in coordination number.²⁵ However, in these milled Ag_3PS_4 samples, disordered structure is dominant. So the decrease in intensity mostly originates from a wider distribution of Ag-S bond length and dynamic distribution, i.e. thermal vibration and ionic diffusion. In the Ag_3PS_4 crystal structure, one Ag^+ ion is coordinated to four $[\text{PS}_4]$ units with the Ag-S bonds.²⁶ Upon high energy milling, the weak Ag-S bonds are broken, and the crystal lattice breaks to give the disordered structure comprised of Ag^+ and $[\text{PS}_4]$ units. By prolonging the mechanical milling, the distribution of Ag-S bond length becomes more and more wide, i.e. the degree of amorphization is continually enhanced.

More importantly, this work gives an insight into the mechanism of formation of amorphization induced by mechanical milling. The mechanical energy generated by milling is transformed into two kinds of energy, which are introduced into the crystalline materials: 1) the potential energy of the system; and 2) thermal energy dissipated in the system.²⁷ In this study, the latter leads to a slight increase in temperature, which is a negligible factor influencing the amorphization. Therefore, in this studied Ag_3PS_4 , the increase in potential energy of the crystalline phase mainly causes the increase in defects and grain boundary area of the crystalline structure. The gradual amorphization occurs from the surface towards the bulk until the entire particle is amorphized. The mechanical milling is so intense that the ions like Ag^+ and the basic structural units like $[\text{PS}_4]$ tetrahedra move from stable to unstable sites with relatively high potential energy, resulting in structural disordering, i.e., amorphization. The mechanical derived-amorphization is a process of breaking the Ag-S bonds, and increasing the distributions of bond angle and bond length. The structure with active Ag^+ ion and disordered $[\text{PS}_4]$ units is likely to possess high ion conductivity.

5. Conclusions

In this work, we successfully synthesized a chalcogenide glass, namely the amorphous Ag_3PS_4 , from its crystalline partner via a high energy ball-milling technique. By performing XRD and DSC measurements for the Ag_3PS_4 samples milled for different durations, we found that a gradual amorphization occurred during milling of the Ag_3PS_4 crystal. By analyzing the change in the non-isothermal crystallization behavior which arises from the surface and bulk crystallization of the particle, it is found that the amorphization occurs from the surface state and extends to the bulk state until complete amorphization of the entire material.

Moreover, the EXAFS spectra indicate that the distribution of Ag-S bond length was broadened and the coordination of Ag ion varied with the increasing duration of the mechanical milling. Therefore, the formation of amorphous Ag_3PS_4 from the crystalline Ag_3PS_4 is a process of amorphization from the surface into the bulk, along with the increasing disorder of the coordination structure.

Acknowledgement

This work was financially supported by NSFC (No.51372180), the Key Technology Innovation Project of Hubei Province (2016AAA029) and Innovation and entrepreneurship leading talent for Yancheng city and Jiangsu province. We acknowledge the provision of synchrotron access to Beamline BL14W1 at the Shanghai Synchrotron Radiation Facility. A Qiao and H Yang contributed equally to this work and should be considered co-first authors.

References

- [1] R. Makiura, T. Yonemura, T. Yamada, M. Yamauchi, R. Ikeda, H. Kitagawa, K. Kato, M. Takata, *Nat. Mater.* **8**(6), 476 (2009).
- [2] I. Valov, I. Sapezanskaia, A. Nayak, T. Tsuruoka, T. Bredow, T. Hasegawa, G. Staikov, M. Aono, R. Waser, *Nat. Mater.* **11**(6), 530 (2012).
- [3] S. Amaresh, K. Karthikeyan, K. J. Kim, Y. G. Lee, Y. S. Lee, *Nanoscale* **6**(12), 6661 (2014).
- [4] D. A. Keen, *J. Phys.: Condens. Matter.* **14**(32), R819 (2002).
- [5] S. Liu, Y. Kong, H. Tao, Y. Sang, *J. Eur. Ceram. Soc.* **37**(2), 715 (2017).
- [6] H. Tao, X. Zhao, Q. Liu, *J. Non-Cryst. Solids.* **377**(10), 146 (2013).
- [7] H. Tao, C. Lin, S. Gu, C. Jing, X. Zhao, *Appl. Phys. Lett.* **91**(1), 475 (2007).
- [8] K. Noi, A. Hayashi, M. Tatsumisago, *J. Power Sources.* **269**, 260 (2014).
- [9] M. H. Enayati, F. A. Mohamed, *Int. Mater. Rev.* **59**(7), 394 (2014).
- [10] G. Dong, H. Tao, X. Xiao, C. Lin, Y. Gong, X. Zhao, S. Chu, S. Wang, *Opt. Express.* **15**(5), 2398 (2007).
- [11] S. S. Berbano, I. Seo, C. M. Bischoff, K. E. Schuller, S. W. Martin, *J. Non-Cryst. Solids.* **358**(1), 93 (2012).
- [12] H. Tao, Z. Yang, P. Lucas, *Opt. Express.* **17**(20), 18165 (2009).
- [13] L. Takacs, *Chem. Soc. Rev.* **42**(18), 7649 (2013).
- [14] D. L. Zhang, *Prog. Mater. Sci.* **49**(3), 537 (2004).
- [15] C. Lin, H. Tao, X. Zheng, R. Pan, H. Zang, X. Zhao, *Opt. Lett.* **34**(4), 437 (2009).
- [16] M. L. Trudeau, R. Schulz, D. Dussault, N. A. Van, *Phys. Rev. Lett.* **64**(1), 99 (1990).
- [17] Z. Zhang, J. H. Kennedy, *J. Electrochem. Soc.* **140**(8), 2384 (1993).
- [18] M. Newville, *J. Synchrotron Radiat.* **8**(2), 322 (2001).
- [19] J. F. Willart, A. D. Gusseme, S. Hemon, G. Odou, F. Danede, M. Descamps, *Solid State Commun.* **119**(8–9), 501 (2001).
- [20] C.C. Tan, L. Lu, A. See, and L. Chan, *J. Appl. Phys.* **91**(5), 2842 (2002).
- [21] C. Suryanarayana, *Prog. Mater. Sci.* **46**(1), 1 (2001).
- [22] S. Chatteraj, C. Bhugra, C. Telang, L. Zhong, Z. Wang, and C. C. Sun, *Pharm. Res.*

- 29**(4), 1020 (2012).
- [23] R. Svoboda, P. Bezdička, J. Gutwirth, J. Málek, *Mater. Res. Bull.* **61**, 207 (2015).
- [24] H. Yamada, I. Saruwatari, N. Kuwata, J. Kawamura, *J. Phys. Chem. C* **118**(41), 23845 (2014).
- [25] J. L. Fulton, S. M. Kathmann, G. K. Schenter, M. Balasubramanian, *J. Phys. Chem. A* **113**(50), 13976 (2009).
- [26] S. Jörgens, A. Mewis, *Solid State Sci.* **9**(2), 213 (2007).
- [27] M.L. Trudeau, R. Schulz, D. Dussault, and N. A. Van, *Phys. Rev. Lett.* **64**(1), 99 (1990).